doi:10.1006/mthe.2001.0475, available online at http://www.idealibrary.com on IDEAL

Quantitative Analysis of Synthetic Gene Delivery Vector Design Properties

Csanad M. Varga,[1,3] Klaudyne Hong,[1,3] and Douglas A. Lauffenburger[1,2,3,*]

[1]*Division of Bioengineering & Environmental Health,* [2]*Department of Chemical Engineering, and* [3]*Biotechnology Process Engineering Center, Massachusetts Institute of Technology, Cambridge, Massachusetts 02139, USA*

**To whom correspondence and reprint requests should be addressed. Fax: (617) 253-2400. E-mail: lauffen@mit.edu.*

As intracellular gene delivery pathways are highly complex combinations of multiple potentially rate-limiting cellular and molecular processes, approaches to the design of synthetic delivery vectors focusing on any single barrier individually will likely be suboptimal. We offer here an "integrative systems" approach to vector characterization and design, combining quantitative experiment and computational modeling studies of vector uptake and trafficking kinetics. This model is validated using data for delivery of a green fluorescent protein (GFP)-encoding plasmid by means of Lipofectamine, permitting specification of model parameter values. The model is then used to make a priori predictions on the effect of polymer length in polyplex vectors, with additional parameter values determined from previous independent experimental studies of plasmid release. Comparison with data on GFP expression via these polyplex vectors shows that the model successfully predicts an experimentally observed biphasic dependence of expression efficiency on polymer length and quantifies the contributions of competing effects yielding the optimal intermediate polymer length. Finally, we use the model to predict potential effects of incorporating nuclear localization sequences in these kinds of synthetic vectors, and find that the degree of benefit from these will depend on the values of other key system properties including the vector unpackaging rate constant. Thus, we demonstrate the usefulness of a bioengineering, integrative-systems modeling approach to improved vector design and analysis.

INTRODUCTION

Despite advantages including selective cell targeting through ligand conjugation, high DNA packaging capacity, manufacturing, and safety, the use of synthetic gene delivery vectors is hampered by transfection efficiencies that are typically much lower than those of their viral counterparts. Accordingly, those currently designing synthetic vectors seek to develop molecular systems mimicking virus-like infection behavior, including cellular attachment and rapid internalization, followed by endosomal escape, nuclear localization, and finally gene expression.

Endocytosis is the predominant mechanism for both synthetic vector and viral uptake and internalization [reviewed in 1]. With the specific and selective targeting of synthetic vectors through the conjugation of targeting moieties onto the vector, receptor-mediated uptake becomes the predominant mechanism. Upon binding to targets on the plasma membrane and internalization, subcellular trafficking can lead to the recycling of complexes to the cell surface or transport to lysosomes for degradation. Based on fundamental understanding of the trafficking behavior of cell receptors, it is possible to maximize the number of internalized vectors through optimization of targeting ligand binding properties such as valency [2]. Therefore, it is possible to manipulate synthetic vector binding and uptake for various targeting ligands and cell types for a desired application.

Subcellular trafficking predominantly leads to transport of internalized complexes through early and late endosomes to lysosomal degradation of the delivered therapeutic [3–9]. Early attempts to overcome this destruction of complexes, at least *in vitro*, consisted of transfecting in the presence of chloroquine to stabilize late endosomes and lysosomes, increasing the probability of intact complex release from these degradative vesicles [4–6,8,10]. This has led to the development of novel polymers and accessory molecules that can offer endosomal escape capabilities, and continues to be the focus of much research in synthetic vector systems [11–16].

Yet cytoplasmic delivery of delivered transgenes is not necessarily sufficient to guarantee substantial levels of gene expression, especially in nondividing cells [8,17–23]. Early work *in vivo* used techniques as drastic as partial hepatectomies to overcome this phenomenon

1525-0016/01 $35.00

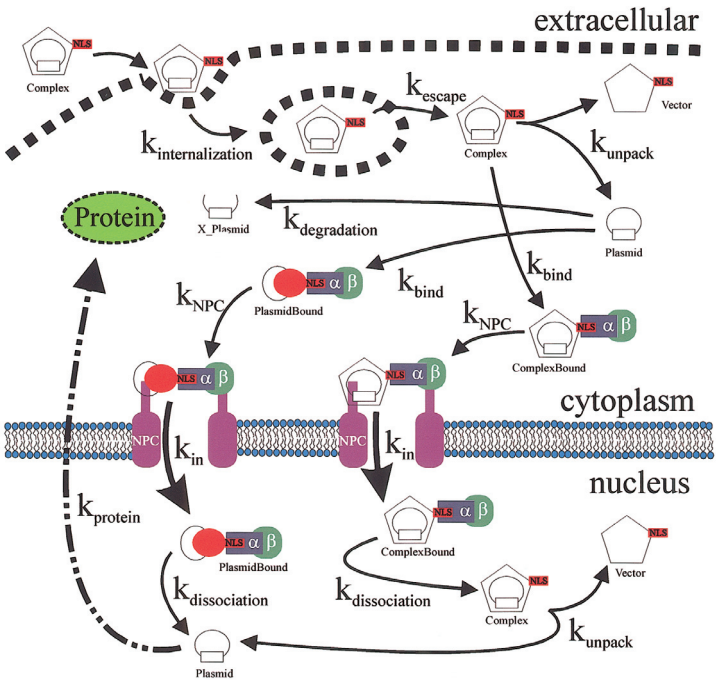

FIG. 1. Schematic diagram of the computational model for gene delivery. Kinetic rate parameters (k_i defined in Table 1) and species (Table 2) are labeled. Successful gene delivery begins with the binding of a complex to the cell surface followed by internalization and requires endosomal escape. The complex can then be imported into the nucleus if the cellular nuclear import machinery binds and associates with nuclear pores. Conversely, the complex may unpackage in the cytoplasm, exposing free plasmids and allowing for nuclear import by a similar mechanism while plasmid degradation simultaneously competes. Within the nucleus, the import machinery must dissociate, and delivered complexes must unpackage to allow for gene expression.

[24]. Because delivered plasmids must translocate into the nucleus for gene transcription to take place, these early techniques served to initiate cell division and cause disruption of the nuclear membrane, increasing the probability of obtaining nuclear plasmids upon reformation of the nuclear membrane.

Substantial effort has been invested into understanding the mechanisms of nuclear uptake of exogenous DNA for cells with intact nuclear membranes, resulting in the creation of synthetic complexes containing nuclear localization sequences (NLSs) similar to those present in their viral counterparts [18,23,25–27]. Because DNA sequences larger than 100 bp are unable to freely diffuse through nuclear pores [28] and most delivered transgenes are 3 kb or larger, nuclear uptake must happen through some facilitated manner through nuclear pore complexes, a process which requires various cytoplasmic factors [21,22,29]. Meanwhile, nucleases present in the cytoplasm serve to rapidly degrade unprotected delivered plasmids [20,30]. Thus, upon cytoplasmic release, it may be necessary to ensure plasmid protection through maintenance of the initial complex until the nuclear translocation machinery can deliver the plasmid and/or complex safely into the nucleus. One potential way to achieve such protection is through control of vector–plasmid dissociation kinetics, termed the "unpackaging rate." It has been shown previously for a polyplex system of epidermal growth factor targeted polylysine that an optimum intermediate polymer length exists corresponding to an optimal unpackaging rate constant that resulted in maximal gene transcription [8]. If unpackaging occurs too readily, cytoplasmic plasmid degradation occurs, whereas if unpackaging occurs too slowly or not at all, the plasmid is inaccessible to the transcriptional machinery.

Lastly, successful nuclear delivery of intact plasmids may not necessarily be sufficient to insure high protein production. Cellular regulation at the level of transcription, translation, and silencing may be involved, as well as the loss of plasmid by dilution in dividing cells [17,19].

Clearly, the cellular processes involved in the route to achieving successful gene delivery are numerous and complex. So, too, are the design parameters available for synthetic vector development. Computational modeling provides a useful tool for analysis and characterization, as well as optimization of such complex systems. Although this kind of approach has, in fact, begun to be used for gene therapy systems, beginning with initial pharmacokinetic models and extending to models of viral attachment and infection [31–35], there are no kinetic models available at the present time focused on characterizing gene delivery processes at the cellular and subcellular levels with the aim of elucidating design principles for how transgene delivery and

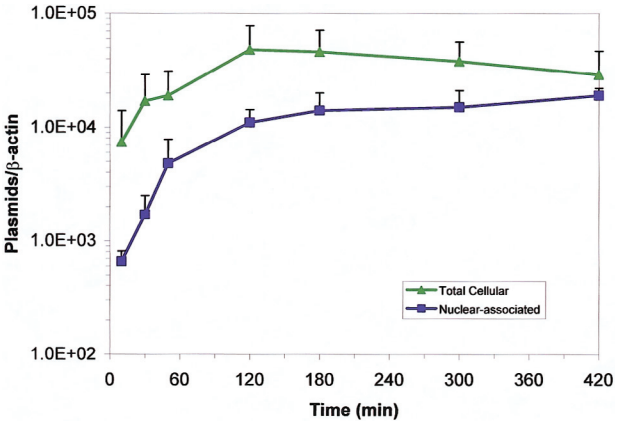

FIG. 2. Experimental internalization and nuclear uptake kinetic data. C3A human hepatoblastoma cells were transfected with a GFP plasmid by means of Lipofectamine, for increasing time periods. At the denoted time points, plasmids were isolated from entire cells or purified nuclei, quantified, and normalized to the endogenous gene, β-actin, using quantitative PCR.

doi:10.1006/mthe.2001.0475, available online at http://www.idealibrary.com on IDEAL

TABLE 1: Model kinetic rate constants

Name	Process	Value determination	Value
$k_{internalization}$	complex internalization	fit, literature [36,37]	see Materials & Methods
k_{escape}	endosomal escape	literature [36,37]	1×10^{-2} min^{-1}
k_{unpack}	vector unpackaging	literature [8,36,37]	1×10^{9} min^{-1}
k_{bind}	formation of nuclear import protein bound vector and/or plasmid	fit from experimental data	2×10^{-3} min^{-1}
k_{NPC}	nuclear pore association	literature [21,22,25,29]	1×10^{3} min^{-1}
k_{In}	nuclear pore import	fit from experimental data	3×10^{-3} min^{-1}
$k_{dissociation}$	import protein dissociation within the nucleus	literature [39]	1×10^{3} min^{-1}
$k_{degradation}$	plasmid degradation	literature [20]	5×10^{-3} min^{-1}
$k_{protein}$	protein production	fit from FACS data (data not shown) [2]	1×10^{-2} min^{-1}

expression vary with quantitative parameters representing molecular, cell, and vector properties. Therefore, a mass action kinetic model was developed containing potentially rate-limiting steps for successful gene delivery including cell/vector binding and internalization, endosomal escape, unpackaging, cytoplasmic degradation, nuclear import, and gene expression (Fig. 1). Kinetic parameters were determined from previous literature reports where available and determined from our own experimental data otherwise. The model was then applied to generate a priori predictions for the effect of polyplex polymer length on transgene expression via its influence on vector/plasmid unpackaging rate; these predictions were successfully tested by comparison with published experimental data [8]. Lastly, we used the model to investigate predicted effects of adding a NLS to a synthetic vector on transgene expression, with the finding that the degree of benefit is highly dependent on values of other key system parameters including the vector unpackaging rate constant.

RESULTS

Kinetics of Vector Uptake: Experimental Data for Lipofectamine-Mediated Delivery

To experimentally examine the kinetics of plasmid internalization, Lipofectamine was used to deliver a GFP-encoding plasmid. We transfected C3A human hepatoblastoma cells at a dose of 2×10^6 plasmids per cell for up to 7 hours. At various time points, transfection was stopped and the cell samples were aliquoted and subjected to total intracellular and nuclear-associated DNA isolation, followed by DNA quantification by real-time PCR. The nuclear-associated fraction consisted of intranuclear and nuclear-membrane-bound plasmids. The determined plasmid numbers for total cellular and nuclear-associated fractions were normalized to the endogenous gene β-actin. Lipid-mediated plasmid internalization was rapid with cytosolic plasmid concentration reaching a peak by 120 minutes, followed by a steady loss of detectable plasmid numbers (Fig. 2). Plasmid translocation through the cytosol toward the nucleus occurred with nuclear-associated plasmids accumulating from 660 plasmids/β-actin at 10 minutes to over 10,000 plasmids/β-actin within 2 hours of transfection.

Validation of a Computational Model Using Lipofectamine Data and Literature Reports

A mechanism-based computational model was constructed containing major potentially rate-limiting processes involved in gene delivery by means of synthetic vectors. These identified barriers include vector/cell binding and internalization, endosomal escape, vector unpackaging, cytoplasmic degradation, nuclear import protein binding, nuclear pore association and import, complex dissociation, and gene expression (Fig. 1). The mathematical model was validated through direct comparison with the experimental data for gene delivery via Lipofectamine (Fig. 2).

Most parameter values were first estimated from relevant previous experimental literature (Table 1). Unpackaging and endosomal escape (k_{unpack} and k_{escape}) were assumed to be instantaneous when coupled to binding and internalization of complexes, as is characteristic of liposomal transfection agents [36,37]. Nuclear import protein binding (k_{bind}) and nuclear pore import (k_{in}) kinetic parameter values were fit to the experimental data and were consistent with values in the literature [21,22,25,29]. Nuclear pore association (k_{NPC}) was assumed to be orders of magnitude faster than nuclear import, as evidenced by the accumulation of excess nuclear membrane associated plasmids in confocal micrographs of labeled plasmids and vectors [8,38]. Plasmid degradation rate constant ($k_{degradation}$) was obtained from kinetic data within the literature [20], whereas complex dissociation ($k_{dissociation}$) within the nucleus was assumed to be rapid, consistent with the mechanism of import protein displacement within the nucleus [39]. Protein production ($k_{protein}$) was determined from FACS experiments (data not shown).

TABLE 2: Model species

Name	Model compartment	Description
$Complex_{Internal}$	cytoplasmic	endosomal complexes
$Complex_{Cytoplasmic}$	cytoplasmic	cytoplasmic complexes
$ComplexBound_{Cytoplasmic}$	cytoplasmic	cytoplasmic import protein bound complexes
$ComplexBound_{NPC}$	nuclear-associated	nuclear pore associated import protein bound complexes
$ComplexBound_{Nuclear}$	nuclear-associated	nuclear import protein bound complexes
$Complex_{Nuclear}$	nuclear-associated	nuclear complexes
$Vector_{Cytoplasmic}$	none	cytoplasmic vectors
$Vector_{Nuclear}$	none	nuclear vectors
$Plasmid_{Cytoplasmic}$	cytoplasmic	cytoplasmic plasmids
$PlasmidBound_{Cytoplasmic}$	cytoplasmic	cytoplasmic import protein bound plasmids
$PlasmidBound_{NPC}$	nuclear-associated	nuclear pore associated import protein bound plasmids
$PlasmidBound_{Nuclear}$	nuclear-associated	nuclear import protein bound plasmids
$Plasmid_{Nuclear}$	nuclear-associated	nuclear plasmids
$X\_Plasmid_{Cytoplasmic}$	none	cytoplasmic degraded plasmids
Protein	none	protein

Given this set of parameter values specified from previous reports, the only remaining model parameters, k_{on} and $k_{internalization}$, were combined and fit from the experimental data (Fig. 2) for total cellular, cytoplasmic, and nuclear-associated plasmid numbers. The resulting model computational results were consistent with crucial features of the experimental data, prominently including the observed saturation of intracellular plasmid numbers and loss of cytoplasmic plasmids to gradual nuclear accumulation and cytoplasmic degradation (Fig. 3). Mathematically, total cellular plasmids included all nondegraded species within the cell, whereas nuclear-associated plasmids included both nuclear-membrane-associated and intranuclear species. The experimental cytoplasmic values represented a subtraction of nuclear-associated from total cellular plasmid numbers, whereas the mathematical values were the sum of non-nuclear, nondegraded intracellular species (Table 2).

Using the model, then, to interpret the Lipofectamine kinetic uptake data, the rapid increase in cytoplasmic plasmids can be attributed to rapid cell binding and internalization, whereas the delayed nuclear association is accounted for by kinetics of nuclear import machinery binding and nuclear pore association. Further, separation of nuclear-associated plasmids into nuclear-membrane-associated and intranuclear plasmids by model analysis revealed at initial time points that less than 1% of nuclear-associated plasmids were intranuclear, however, by 7 hours intranuclear plasmids constituted 66% of nuclear-associated plasmids (data not shown). Finally, plasmid number decrease can be attributed to cytoplasmic degradation of delivered plasmids.

A Priori Computational Model Predictions: Effect of Polyplex Polymer Chain Length

The computational model was then applied to generate a priori predictions for the effect of the vector unpackaging rate constant, as governed by the length of a polymer in a polyplex delivery vector. It has been found that varying polylysine chain length influences the unpackaging rate, with an intermediate chain length yielding maximal gene expression [8]. In those experiments, NIH 3T3 fibroblast cells were transfected with epithelial growth factor (EGF)-targeted polylysine of three different polymer chain lengths complexed with a plasmid encoding green fluorescent protein (GFP), in the presence of the endosomalytic agent chloroquine to aid endosomal escape by the polyplex vector. The respective vector/plasmid complex unpackaging rates were determined experimentally *in vitro*, and the corresponding GFP expression efficiencies and levels were measured at 48 hours post-transfection, for each of the three polylysine chain lengths. Greatest expression was found for the intermediate chain length, which exhibited an intermediate unpackaging rate compared with the smaller and larger polymers.

To test whether our model could predict these findings, the model unpackaging rate constant was varied across a range of values including those corresponding to the experimental measurements for the three polylysine vector chain lengths. All other model parameter values were held constant, according to the assumption that the 3T3 cells and C3A cells possess roughly similar trafficking and nuclear translocation properties for synthetic vectors lacking specific NLSs. The use of chloroquine in the polylysine experiments is a reasonable justification for assuming that the endosomal escape rate constant for the polylysine vector is similar to that for the Lipofectamine vector. The computational value for GFP production was normalized to the maximal value for direct comparison with experimental data. The computational model successfully predicts the biphasic dependence of transgene expression on the vector unpackaging rate constant (Fig. 4). Moreover, it successfully predicts the approximate value of the

doi:10.1006/mthe.2001.0475, available online at http://www.idealibrary.com on IDEAL

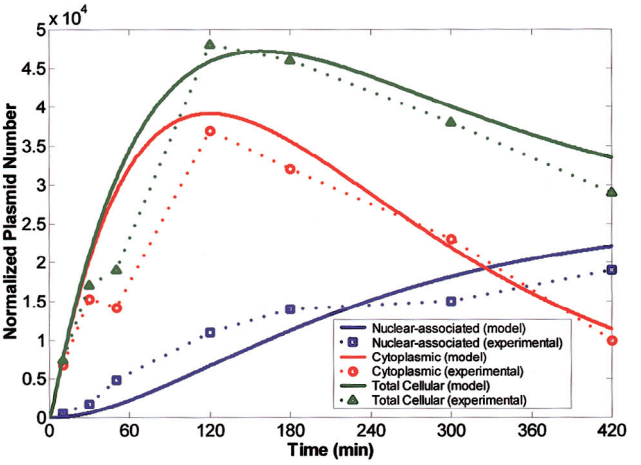

FIG. 3. Model prediction of internalization and nuclear uptake kinetics. Experimental data are from Fig. 2, and model computations use the set of parameter values listed in Table 1.

optimal intermediate value for the unpackaging rate constant for the situation characterized by this set of other system parameter values. It must be emphasized that these predictions involved no fitting of additional parameters; all had been specified previously from independent data or estimates.

Beyond the benefit of purely numerical prediction of the experimentally observed phenomenon, the computational model can be used to interpret in more depth the reasons underlying this biphasic dependence. Parametric sensitivity analysis revealed that unpackaging, plasmid degradation, and nuclear import machinery binding are, in this situation, the key processes controlling nuclear delivery of intact plasmids and ultimate expression (data not shown). Thus, it is the tradeoff between unpackaging too quickly, increasing cytosolic degradation of the plasmid DNA relative to nuclear import, and unpackaging too slowly, inhibiting intranuclear release for transcription, that governs the optimal unpackaging rate for this polyplex vector.

DISCUSSION

Current efforts in synthetic vector gene delivery research have primarily focused on the development of systems designed to address particular individual barriers to efficient gene delivery in an isolated rather than an integrated fashion. At the cellular level, these barriers include, but are not limited to, inefficient vector/cell binding and internalization, subcellular trafficking for degradation by lysosomes related to poor endosomal escape characteristics, degradation by cytoplasmic nucleases, nuclear import, vector unpackaging, and gene expression (Fig. 1). However, as vectors are developed that overcome a potentially limiting step, other barriers can in turn become predominant. Therefore, a multi-parameter systems analysis based on quantitative methodologies should be useful for designing and fully characterizing synthetic vectors. Such quantitative techniques serve to facilitate vector evolution through identification of rate-limiting barriers as they relate to cellular and vector parameters. Mechanistic level multiple vector comparisons can be performed, providing insight into molecular attributes yielding efficient gene delivery. Using such information, rational design of novel vectors becomes possible. The questions evolve from asking if one vector works better than another, where relative light units or GFP expression is considered the metric of gene delivery success, to asking why, where, and how one vector works better than another.

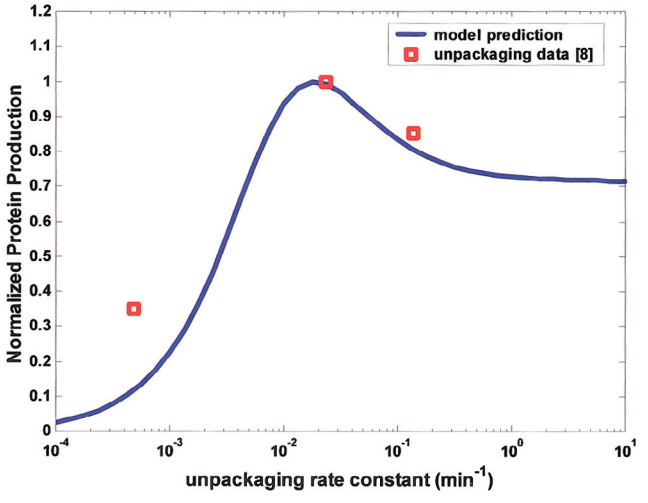

Computational modeling offers a powerful tool for such systems-based investigation. Imperative for the development and implementation of models is founding their basis in quantitative experimental techniques. Real-time PCR allows for the direct measure of plasmid levels from cells and subcellular compartments, and we have used it here in combination with literature data to help validate our model. Transfection of C3A cells with a GFP plasmid by means of Lipofectamine resulted in a rapid increase in total cellular plasmids, with delayed nuclear association (Fig. 2). Cellular uptake reached a maximum at 120 minutes, after which saturation of uptake occurred and plasmids were lost to cytoplasmic degradation. Nuclear association and uptake followed with a delay correlating to import protein binding and nuclear pore association.

The mass-action model we constructed allows unbiased incorporation of multiple processes represented

FIG. 4. Effect of varying synthetic vector polymer length on protein production. Model computations use the set of parameter values listed in Table 1, with the unpackaging rate constant varied across a range from very slow to very fast. Experimental data points are from Schaffer *et al.* [8] for NIH 3T3 cells transfected with a GFP plasmid via polylysine vectors of three different chain lengths.

by kinetic rate constants parameters (Table 1) with intermediate species (Table 2) into a set of differential equations. As such, the model parameters are independent and of equal weight mathematically. Further, through sensitivity analyses, model dependences on specific parameters over time can be identified, allowing for identification of the dominant rate-limiting cellular process at any time. All model parameter values were estimated from relevant previous experimental reports, except the vector binding and internalization rate constants (Table 1). These latter two were combined and determined by fitting computational results to our experimental cellular uptake and nuclear association kinetics of the Lipofectamine-delivered plasmid DNA (Fig. 3). Using the model, it was possible to investigate the contribution of nuclear-membrane-bound versus intranuclear contributions to the experimental nuclear-associated numbers. Intranuclear plasmids accounted for less than 1% of nuclear-associated plasmids at the earliest time point and 66% of the nuclear-associated plasmids by 7 hours (data not shown). This further supports the evidence that nuclear import of plasmid DNA may be a potentially rate-limiting step for many applications [18,21–23,25–30].

Vector unpackaging has been shown to have an optimal intermediate value for maximal gene expression [8], based on experiments transfecting NIH 3T3 fibroblasts with EGF-targeted polylysine of various polymer chain lengths complexed with a plasmid encoding GFP. Complex unpackaging was measured *in vitro* for the chain lengths tested and correlated to GFP expression at 48 hours post transfection [8]. With all other model parameters now specified, we varied the vector unpackaging rate constant across a range including the experimentally determined values; thus, the computational model predictions are a priori in nature, and involve no fitting of additional parameters from the new data set. The comparison between model computations and experimental results (Fig. 4) demonstrates that the model successfully predicts not only the qualitative nature of the biphasic dependence of transgene expression on vector unpackaging rate but also the quantitative value of the intermediate unpackaging rate constant that yields maximal expression. It must be noted, of course, that some disparities may arise from any errors due to using model parameter values (except for the unpackaging rate constant) determined or estimated from cell systems different from the NIH 3T3 cells used in the previous study [8]. The assumption that endosomal escape and nuclear import rate constants for Lipofectamine and polylysine (in the presence of the endosomolytic agent chloroquine) are similar may also contribute to the model prediction deviation from the experimental values.

Beyond this sort of particular hypothesis testing, an even broader impact of the computational model should lie in its ability to explore potential effects of vector parameters on gene delivery in a multiparameter space, for purposes of improved vector design. The complexity of mechanisms resulting in efficient gene delivery requires such an integrated-systems perspective. Because nuclear import has been a major focus of numerous experimental vector development efforts, we further applied our computational model to investigate the potential effects of inclusion of NLSs in plasmid trafficking and expression. The value of the nuclear import protein binding constant was varied along with that of the unpackaging rate constant, simulating conjugation to synthetic vectors of different polymer chain lengths with NLSs having increasing affinities to the nuclear import machinery, while the remaining model parameters were held constant. Computational results are illustrated in Fig. 5. The model predicts a "threshold" unpackaging rate constant of 10^{-3} min^{-1}, below which enhancement of nuclear import machinery binding has little to no effect on transgene expression. At the same time, analysis of model results (data not shown) revealed an

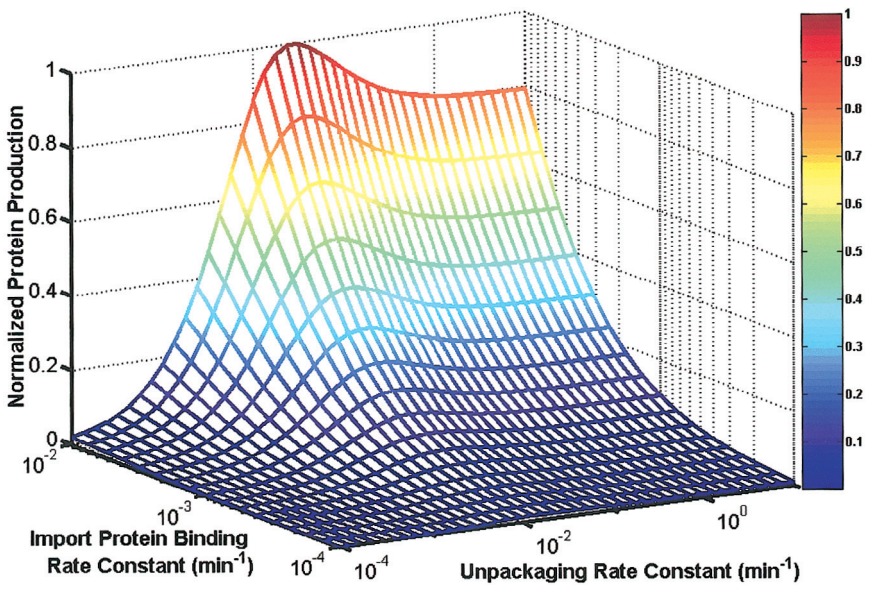

FIG. 5. Model prediction of NLS incorporation onto a synthetic vector. NLS addition of increasing affinities was simulated by increasing the import protein machinery binding constant. The model was computed in conjunction with varying unpackaging rate (other parameter values listed in Table 1) to simulate addition of NLSs on synthetic vectors of decreasing polymer chain length (increasing unpackaging rate constant).

doi:10.1006/mthe.2001.0475, available online at http://www.idealibrary.com on IDEAL

increase in nuclear delivery of plasmids still complexed with the vector. Above the threshold unpackaging rate constant, NLS addition should indeed yield a substantial increase in nuclear plasmid delivery and protein production. The threshold unpackaging rate constant seems to represent a lower limit value for polyplex gene delivery such that adding a NLS will not have a significant affect on protein production. That is, if the vector can unpackage from the plasmid only very slowly, the DNA is not accessible for transcription even if there is an increase in nuclear delivery of the complex facilitated by the NLS.

Therefore, this model simulation represents the experimental addition of NLSs of varying affinities to a polymer vector while simultaneously determining the optimal chain length. Intuitively, addition of a NLS should increase nuclear uptake of delivered plasmids and should therefore cause a corresponding increase in gene expression. However, the model predicted a significant increase in gene expression only above a threshold unpackaging rate of 10^{-3} min^{-1}. Upon reconsideration, such a phenomenon makes sense; if the vector does not unpackage sufficiently, thereby inhibiting transcription initiation by protecting the DNA from the transcription machinery, no amount of nuclear plasmid delivery augmentation will increase gene expression. Model analysis reveals that, for example, at the threshold unpackaging rate constant (k_{unpack}) value of 10^{-3} min^{-1}, conjugation of a NLS onto the vector—effectively increasing the import protein binding rate constant (k_{bind}) from 10^{-3} min^{-1} to 10^{-2} min^{-1}—is predicted to increase normalized protein production from approximately 8% to 18% of the maximal value, whereas the same NLS conjugation to a vector with the optimal unpackaging rate constant of 10^{-2} min^{-1} is predicted to increase normalized protein production from approximately 14% to 100% of the maximum value. Yet, with the vast number of potential parameter combinations, many of which are not so intuitive, it is easy to see how the myriad of design characteristics available for synthetic vector development can be incorrectly applied or left unoptimized.

Although the developed model successfully predicts the *in vitro* uptake and trafficking of liposomal and polylysine delivered plasmids, it is insufficient to correlate to *in vivo* work. However, *in vivo* correlation may result from further development of the mathematical model to include equations and parameters describing events and processes involved with complex administration to the animal including, but certainly not limited to, delivery of complexes directly to tissues or intravenously, blood transport and component interaction, transport to organs, systemic clearance, diffusion through tissues, and cell binding. Such further model developments may be instrumental in characterizing gene delivery treatment behavior and perhaps in reducing or refining *in vivo* expermentation.

Further model validation will come from its application to other cell types and vector systems, viral and nonviral, as the processes occurring for synthetic vectors must also occur for their viral counterparts. Such application of the model will require quantitative, dynamic experimental data on cell and vector properties.

MATERIALS AND METHODS

Construction of computational model. A first-order mass action kinetic model was constructed for gene delivery (Fig. 1). Included in this model are the processes of vector/cell binding and internalization, endosomal escape, vector unpackaging, plasmid degradation in the cytoplasm, nuclear import protein binding, nuclear pore complex association and import, import protein dissociation, and protein production. This essentially represents the simplest computational model capable of accounting for the key processes previously reported to significantly influence transgene delivery and expression via synthetic vectors [1]. Increased complexity can be incorporated by including nonlinearities in a number of the rate processes, if appropriate quantitative experimental information is available.

Model kinetic parameters (Table 1) and species (Table 2) were combined to derive the following ordinary differential equations (ODEs) and solved simultaneously using a stiff ODE solver in MATLAB (The MathWorks, Inc., Natick, MA), where each equation is the differential mass balance for a particular species. The initial conditions for all species were set at zero plasmids; the cells were assumed to be at a steady-state in the absence of any plasmid, vector, or complex before the addition of transfection complexes.

$$d(Complex_{Internal})/dt = Complex_{total} * e^{(-t)} - k_{escape} * Complex_{Internal} \quad (1)$$

$$d(Complex_{Cytoplasmic})/dt = k_{escape} * Complex_{Internal} - k_{bind} * Complex_{Cytoplasmic} - k_{unpack} * Complex_{Cytoplasmic} \quad (2)$$

$$d(ComplexBound_{Cytoplasmic})/dt = k_{bind} * Complex_{Cytoplasmic} - k_{NPC} * ComplexBound_{Cytoplasmic} \quad (3)$$

$$d(ComplexBound_{NPC})/dt = k_{NPC} * ComplexBound_{Cytoplasmic} - k_{In} * ComplexBound_{NPC} \quad (4)$$

$$d(ComplexBound_{Nuclear})/dt = k_{In} * ComplexBound_{NPC} - k_{dissociation} * ComplexBound_{Nuclear} \quad (5)$$

$$d(Complex_{Nuclear})/dt = k_{dissociation} * ComplexBound_{Nuclear} - k_{unpack} * Complex_{Nuclear} \quad (6)$$

$$d(Vector_{Nuclear})/dt = k_{unpack} * Complex_{Nuclear} + k_{dissociation} * VectorBound_{Nuclear} \quad (7)$$

$$d(Plasmid_{Nuclear})/dt = k_{unpack} * Complex_{Nuclear} + k_{dissociation} * PlasmidBound_{Nuclear} \quad (8)$$

$$d(Vector_{Cytoplasmic})/dt = k_{unpack} * Complex_{Cytoplasmic} - k_{bind} * Vector_{Cytoplasmic} \quad (9)$$

$$d(Plasmid_{Cytoplasmic})/dt = k_{unpack} * Complex_{Cytoplasmic} - k_{bind} * Plasmid_{Cytoplasmic} - k_{degradation} * Plasmid_{Cytoplasmic} \quad (10)$$

$$d(PlasmidBound_{Cytoplasmic})/dt = k_{bind} * Plasmid_{Cytoplasmic} - k_{NPC} * PlasmidBound_{Cytoplasmic} \quad (11)$$

$$d(PlasmidBound_{NPC})/dt = k_{NPC} * PlasmidBound_{Cytoplasmic} - k_{In} * PlasmidBound_{NPC} \quad (12)$$

$$d(PlasmidBound_{Nuclear})/dt = k_{In} * PlasmidBound_{NPC} - k_{dissociation} * PlasmidBound_{Nuclear} \quad (13)$$

$$d(X\_Plasmid_{Cytoplasmic})/dt = k_{degradation} * Plasmid_{Cytoplasmic} - k_{bind} * X\_Plasmid_{Cytoplasmic} \quad (14)$$

$$d(Protein)/dt = k_{protein} * Plasmid_{Nuclear} \quad (15)$$

Equation (1), the mass ODE for the number of internalized complexes ($Complex_{Internal}$), was derived using the parameter $Complex_{total}$, the total number of plasmids delivered to a cell, fit from the experimental data to a value of 9.0×10^4 plasmids. This equation captured the saturation of uptake and escape of plasmids into the cytoplasm observed experimentally at the total delivered complex number, a process not simply described by an internalization parameter ($k_{internalization}$).

The parameter values (Table 1) are first-order rate constants representing cellular and vector processes and therefore have units of min^{-1}. When the inverse of the value is multiplied by the natural log of 2, a characteristic half-life for the process may be obtained. For example, the characteristic half-life for plasmid degradation in the cytoplasm, the natural log of 2 divided by $k_{degradation}$, yields 138 min, or approximately 2 h.

TaqMan real-time quantitative PCR. Plasmid quantification was carried out using the PE Biosystems Prism 7700 (PE Biosystems, Foster City, CA). For GFP and β-actin amplifications, forward and reverse primers were accompanied by a TaqMan probe nestled between the primers. The probe contained a 3′ quencher and a 5′ fluorescent dye, which was cleaved and released by the 5′ to 3′ exonuclease activity of AmpliTaq Gold polymerase during primer extension. The freed fluorescent signals were detected by a CCD camera, allowing real-time accumulation of amplification signals at each cycle. An increase in fluorescence signal was possible only if the target sequence had triple primer and probe sequence complementarity (all reagents PE Biosystems, Foster City, CA).

The GFP product was 72 bp and the β-actin control, 295 bp. Both GFP and β-actin probes were oligonucleotides containing a 3′ TAMRA quencher molecule attached via a linker arm and a 5′ covalently linked FAM or VIC fluorescent dye. The 3′ end of the probe was blocked to prevent extension of the probe during PCR. The GFP primer and probe sequences were designed with Primer Express software (PE Biosystems, Foster City, CA): forward primer F1 (5′-CCACTACCTGAGCACCCAGTC-3′), reverse primer R1 (5′-TCCAGCAGGACCATGTGATC-3′), and probe P1 (5′-CCCTGAGCAAAGACCCCAACGAGAA-3′). The β-actin primers and probe (PE Biosystems, Foster City, CA) were as follows: forward primer (5′-TCACCCACACTGTGCCCATCTACGA-3′), reverse primer (5′-CAGCGGAACCGCTCATTGCCAATGG-3′), and probe (5′-ATGCCCTCCCCCATGCCATCCTGCGT-3′).

SYBR Green real-time PCR of GFP standards was also carried out for comparison with probe. To prevent PCR carryover contamination, dUTP substituted for dTTP during PCR such that all previously amplified templates containing dUTP would be cleaved by uracil *N*-glycosylase (UNG), which also degraded any misprimed, nonspecific products during the 50°C incubation step before amplification. The PCR cycle conditions were 50°C for 2 min and 95°C for 10 min, followed by 40 cycles of 95°C for 15 s and 60°C for 1 min.

Plasmid DNA, vector, and cell line. Plasmid pEGFP-C1 (Clontech, Palo Alto, CA) encodes a red-shifted variant of wild-type GFP optimized for brighter fluorescence and higher expression in mammalian cells with excitation maximum at 488 nm and emission maximum at 507 nm. Expression is controlled by the human cytomegalovirus (CMV) immediate early promoter, enhancer region, and TATA box. For propagation in *Escherichia coli*, 500 ng of plasmid was heat-shocked at 42°C into *E. coli* competent cells. The plasmid DNA was purified using a plasmid maxi prep, according to the manufacturer's instructions (Qiagen, Valencia, CA). Lipofectamine reagent (Gibco BRL, Rockville, MD) is a 3:1 (w/w) liposome formulation of the polycationic lipid 2,3-dioleyloxy-*N*-[2(sperminecarboxamido)ethyl]-*N*,*N*-dimethyl-1-propanaminium trifluoroacetate (DOSPA; Chemical Abstracts Registry name: *N*-[2-({2,5-bis[(3-aminopropyl)amino]-1-oxypentyl}amino)ethyl]-*N*,*N*-dimethyl-2,3-bis(9-octadecenyloxy)-1-propanaminium trifluoroacetate), and the neutral lipid dioleoyl phosphatidylethanolamine (DOPE) in membrane filtered water. Each molecule of DOSPA has five positive charges.

C3A hepatoblastoma cell line (ATCC) was derived from HepG2, an epithelial cell line originated from a 15-year-old male Caucasian. It was cultured in modified essential medium (MEM) supplemented with 10% fetal bovine serum (FBS; both reagents from ATCC), at 37°C and 5% CO_2. An antibody against SV40 large T-antigen (Chemicon, Temecula, CA) confirmed that C3A was SV40-negative and unable to replicate pEGFP-C1 plasmid DNA.

Transfection, FACS, and DNA isolation. For transfection, cells in 35 mm Corning plates (VWR, Boston, MA) were washed once with serum-free medium (SFM). DNA-lipid complexes were added to cells and re-incubated. Transfection was interrupted with extracellular plasmids diluted and removed by double PBS washes, followed by cellular trypsinization, centrifugation, and a third PBS wash. Nuclei isolation followed a standard protocol whereby 0.5% (v/v) NP-40 in a buffer supplemented with 10 mM TrisCl, pH 7.4, and 3 mM $MgCl_2$ was twice used to achieve cell lysis and the nuclear pellet centrifuged and purified away from supernatant that contained cytosolic plasmids and cellular debris [40]. DNA purification from either purified nuclei or whole cells proceeded with Triton X-100, RNase, Proteinase K, and phenol: chloroform: isoamylalcohol (25:24:1); DNA was precipitated with ethanol and 0.3 M sodium acetate (all reagents Sigma, St. Louis, MO).

ACKNOWLEDGMENTS

We thank Tom Wickham (GenVec, Inc.) for helpful comments and suggestions. This work was supported by the National Science Foundation Engineering Research Center program and a Whitaker Foundation Graduate Fellowship to C.V.

RECEIVED FOR PUBLICATION JUNE 13; ACCEPTED AUGUST 31, 2001.

REFERENCES

1. Varga, C. M., Wickham, T. J., and Lauffenburger, D. A. (2000). Receptor-mediated targeting of gene delivery vectors: insights from molecular mechanisms for improved vehicle design. *Biotechnol. Bioeng.* **70:** 593–605.
2. Schaffer, D. V., and Lauffenburger, D. A. (1998). Optimization of cell surface binding enhances efficiency and specificity of molecular conjugate gene delivery. *J. Biol. Chem.* **273:** 28004–28009.
3. Buschle, M., *et al.* (1995). Receptor-mediated gene transfer into human T lymphocytes *via* binding of DNA/CD3 antibody particles to the CD3 T cell receptor complex. *Hum. Gene Ther.* **6:** 753–761.
4. Choi, Y. H., Liu, F., Park, J. S., and Kim, S. W. (1998). Lactose-poly(ethylene glycol)-grafted poly-L-lysine as hepatoma cell-targeted gene carrier. *Bioconj. Chem.* **9:** 708–718.
5. Cotten, M., *et al.* (1990). Transferrin-polycation-mediated introduction of DNA into human leukemic cells: Stimulation by agents that affect the survival of transfected DNA or modulate transferrin receptor levels. *Proc. Natl. Acad. Sci. USA* **87:** 4033–4037.
6. Erbacher, P., *et al.* (1996). Gene transfer by DNA/glycosylated polylysine complexes into human blood monocyte-derived macrophages. *Hum. Gene Ther.* **7:** 721–729.
7. Furs, S., and Wu, G. Y. (1994). Receptor-mediated targeted gene delivery using asialoglycoprotein-polylysine conjugates. In *Gene Therapeutics: Methods and Applications of Direct Gene Transfer* (J. A. Wolff, Ed.) pp. 382–390. Birkhauser, Boston.
8. Schaffer, D. V., Fidelman, N. A., Dan, N., and Lauffenburger, D. A. (2000). Vector unpacking as a potential barrier for receptor-mediated polyplex gene delivery. *Biotechnol. Bioeng.* **67:** 598–606.
9. Wagner, E., Curiel, D., and Cotten, M. (1994). Delivery of drugs, proteins and genes into cells using transferrin as a ligand for receptor-mediated endocytosis. *Adv. Drug Deliv. Rev.* **14:** 113–135.
10. Zenke, M., *et al.* (1990). Receptor-mediated endocytosis of transferrin-polycation conjugates: an efficient way to introduce DNA into hematopoietic cells. *Proc. Natl. Acad. Sci. USA* **87:** 3655–3659.
11. Abdallah, B., *et al.* (1996). A powerful nonviral vector for in vivo gene transfer into the adult mammalian brain: polyethylenimine. *Hum. Gene Ther.* **7:** 1947–1954.
12. Boussif, O., *et al.* (1995). A versatile vector for gene and oligonucleotide transfer into cells in culture and in vivo: polyethylenimine. *Proc. Natl. Acad. Sci. USA* **92:** 7297–7301.
13. Gonzales, H., Hwang, S. J., and Davis, M. E. (2000). A new class of polymers for the delivery of macromolecular therapeutics. *Bioconj. Chem.* **10:** 1068–1074.
14. Putnam, D., Gentry, C. A., Pack, D. W., and Langer, R. (2001). Polymer-based gene delivery with low cytotoxicity by a unique balance of side-chain termini. *Proc. Natl. Acad. Sci. USA* **98:** 1200–1205.
15. von Harpe, A., Petersen, H., Li, Y., and Kissel, T. (2000). Characterization of commercially available and synthesized polyethylenimines for gene delivery. *J. Control. Release* **69:** 309–322.
16. Zanta, M.-A., Boussif, O., Adib, A., and Behr, J.-P. (1997). In vitro gene delivery to hepatocytes with galactosylated polyethylenimine. *Bioconj. Chem.* **8:** 839–844.
17. Brunner, S., *et al.* (2000). Cell cycle dependence of gene transfer by lipoplex, polyplex and recombinant adenovirus. *Gene Ther.* **7:** 401–407.
18. Ciolina, C., *et al.* (1999). Coupling of nuclear localization signals to plasmid DNA and specific interaction of the conjugates with importin a. *Bioconj. Chem.* **10:** 49–55.
19. Hong, K. (2000). Cellular *de novo* methylation of plasmid DNA and internalized plasmid numbers: effects on lipid vector gene delivery and expression. Thesis, MIT, Boston, MA.
20. Lechardeur, D., *et al.* (1999). Metabolic instability of plasmid DNA in the cytosol: a potential barrier to gene transfer. *Gene Ther.* **6:** 482–497.
21. Vacik, J., Dean, B. S., Zimmer, W. E., and Dean, D. A. (1999). Cell-specific nuclear import of plasmid DNA. *Gene Ther.* **6:** 1006–1014.
22. Wilson, G. L., Dean, B. S., Wang, G., and Dean, D. A. (1999). Nuclear import of plasmid DNA in digitonin-permeabilized cells requires both cytoplasmic factors and specific DNA sequences. *J. Biol. Chem.* **274:** 22025–22032.
23. Zanta, M. A., Belguise-Valladier, P., and Behr, J.-P. (1999). Gene delivery: a single nuclear localization signal peptide is sufficient to carry DNA to the cell nucleus. *Proc. Natl. Acad. Sci. USA* **96:** 91–96.
24. Wu, G. Y., *et al.* (1991). Receptor-mediated gene delivery in vivo. *J. Biol. Chem.* **266:** 14338–14342.
25. Chan, C. K., and Jans, D. A. (1999). Enhancement of polylysine-mediated transferrinfection by nuclear localization sequences: polylysine does not function as a nuclear localization sequence. *Hum. Gene Ther.* **10:** 1695–1702.
26. Subramanian, A., Ranganathan, P., and Diamond, S. L. (1999). Nuclear targeting peptide scaffolds for lipofection of nondividing mammalian cells. *Nat. Biotechnol.* **17:** 873–877.

doi:10.1006/mthe.2001.0475, available online at http://www.idealibrary.com on IDEAL

27. Tachibana, R., *et al.* (1998). Intracellular regulation of macromolecules using pH-sensitive liposomes and nuclear localization signal: qualitative and quantitative evaluation of intracellular trafficking. *Biochem. Biophys. Res. Commun.* **251:** 538–544.
28. Ludtke, J. J., Zhang, G., Sebestyen, M. G., and Wolff, J. A. (1999). A nuclear localization signal can enhance both the nuclear transport and expression of 1kb DNA. *J. Cell Sci.* **112:** 2033–2041.
29. Dean, D. A. (1997). Import of plasmid DNA into the nucleus is sequence specific. *Exp. Cell Res.* **230:** 293–302.
30. Zabner, J., Fasbender, A. J., Moninger, T., Poellinger, K. A., and Welsh, M. J. (1995). Cellular and molecular barriers to gene transfer by a cationic lipid. *J. Biol. Chem.* **270:** 18997–19007.
31. Andreadis, S. T., and Palsson, B. O. (1996). Kinetics of retrovirus mediated gene transfer: the importance of intracellular half-life of retroviruses. *J. Theor. Biol.* **182:** 1–20.
32. Ledley, T. S., and Ledley, F. D. (1994). Multicompartment, numerical model of cellular events in the pharmacokinetics of gene therapies. *Hum. Gene Ther.* **5:** 679–691.
33. Wickham, T. J., Granados, R. R., Wood, H. A., Hammer, D. A., and Shuler, M. L. (1990). General analysis of receptor-mediated viral attachment to cell surfaces. *Biophys. J.* **58:** 1501–1516.
34. Wickham, T. J., Shuler, M. L., and Hammer, D. A. (1995). A simple model to predict the effectiveness of molecules that block attachment of human rhinoviruses and other viruses. *Biotechnol. Prog.* **11:** 164–170.
35. Dee, K. U., and Shuler, M. L. (1997). A mathematical model of the trafficking of acid-dependent enveloped viruses: application to the binding, uptake, and nuclear accumulation of baculovirus. *Biotechnol. Bioeng.* **54:** 468–490.
36. Zelphati, O., and Szoka, F. (1996). Mechanism of oligonucleotide release from cationic liposomes. *Proc. Natl. Acad. Sci. USA* **93:** 11493–11498.
37. Lappalainen, K., Miettinen, R., Kellokoski, J., Jaaskelainen, I., and Syrjanen, S. (1997). Intracellular distribution of oligonucleotides delivered by cationic liposomes: light and electron microscopic study. *J. Histochem. Cytochem.* **45:** 265–274.
38. Godbey, W. T., Wu, K., and Mikos, A. G. (1999). Tracking the intracellular path of poly(ethylenimine)/DNA complexes for gene delivery. *Proc. Natl. Acad. Sci. USA* **96:** 5177–5181.
39. Moroianu, J., Blobel, G., and Radu, A. (1996). Nuclear protein import: Ran-GTP dissociates the karyopherin ab hererodimer by displacing a from an overlapping binding site on b. *Proc. Natl. Acad. Sci. USA* **93:** 7059–7062.
40. Greenberg, M. E., and Bender, T. P. (1997). Identification of newly transcribed RNA. *Curr. Prot. Mol. Biol.* **1:** 4.10.11–14.10.11.